Eddy Sensitivity to Jet Characteristics

JANNI YUVAL AND YOHAI KASPI

Department of Earth and Planetary Sciences, Weizmann Institute of Science, Rehovot, Israel

(Manuscript received 3 May 2017, in final form 25 January 2018)

ABSTRACT

The atmosphere exhibits two distinct types of jets: the thermally driven subtropical jet and the more poleward eddy-driven jet. Depending on location and season, these jets are often merged or separated, and their position, structure, and intensity strongly influence the eddy fields. Here, the authors study the sensitivity of eddies to changes in the jets' amplitudes and positions in an idealized general circulation model. A modified Newtonian relaxation scheme that has a very short relaxation time for the mean state and a long relaxation time for eddies is used. This scheme makes it possible to obtain any zonally symmetric temperature distribution and is used to systematically modify the jets' amplitudes and locations. It is found that eddies are more sensitive to changes in the amplitude of the eddy-driven jet than to changes in the amplitude of the subtropical jet. Furthermore, when the eddy-driven jet is shifted poleward, eddies tend to intensify. These results are tested for robustness in two different reference simulations: one resembling a situation where the subtropical and eddy-driven jets are nearly merged and one when they are separated.

1. Introduction

The current understanding is that two types of jets exist in the atmosphere: a subtropical jet (STJ) and an eddy-driven jet (EDJ), also referred to in the literature as the subpolar jet. Two different mechanisms are responsible for the existence of these jets. The STJ is primarily driven by the advection of planetary angular momentum by the thermally direct Hadley circulation (Held and Hou 1980), and eddies usually act to weaken this jet. On the other hand, the EDJ is driven by eddy momentum flux convergence (EMFC), which accelerates the zonal-mean westerly wind (Held 1975; Rhines 1975; Panetta 1993).

Since these jets are a result of different processes, the locations of these jets are different. The STJ is located at the edge of the Hadley cell, while the EDJ is located inside the Ferrel cell, where the EMFC is maximal. In practice, there are different regimes for the atmospheric jets, and both jets are not always present or cannot always be clearly distinguished. For example, in the summer hemisphere when the Hadley cell is very weak, the STJ typically does not exist, and there is a relatively weak EDJ. In transition seasons and winter, when the Hadley cell is present, there are two possible regimes: (i) two well-separated jets as in the northern Atlantic in January where EMFC is found only in the vicinity of the EDJ [Fig. 1a herein and also in Eichelberger and Hartmann (2007)] and (ii) a single merged (mixed) jet as in the northern Pacific in January, which is driven both from thermally direct Hadley cell in its more equatorward regions and by EMFC in its poleward flank (Fig. 1b). In addition, the STJ and the EDJ are distinguished by their vertical structures. The STJ is more baroclinic and has very weak surface winds below its maximum, while the EDJ is more barotropic, and surface westerlies are located below its maximum to balance the upper-tropospheric EMFC (Vallis 2006).

A number of previous studies investigated the relationship between the jet characteristics and eddies. Lee and Kim (2003) used linear stability analysis to show that when a weak STJ is present and the Eady growth rate (Eady 1949) is maximal poleward of the jet peak, the growth of eddies will occur 20°–30° poleward of the STJ, and a second jet (an EDJ) will emerge. On the other hand, when the STJ is strong and baroclinicity peaks close to its core, eddies will grow in its vicinity and only a single (merged) jet will be present. Consistent with this result, Son and Lee (2005) showed in an idealized GCM with a Newtonian relaxation scheme that a double-jet state is favored when the STJ is weak and the baroclinic zone is wide. In a different study, Nakamura and Sampe (2002) used reanalysis data to show that when the STJ is strong above the Pacific, it can trap eddy activity within its core, away from the strong sea surface temperature (SST)

Corresponding author: Janni Yuval, yaniyuval@gmail.com

DOI: 10.1175/JAS-D-17-0139.1

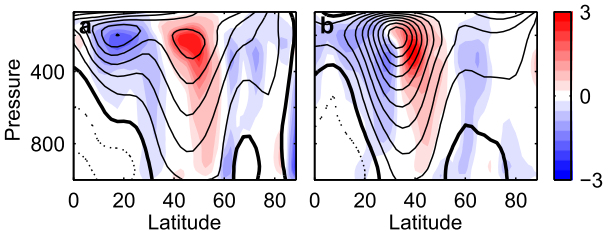

FIG. 1. Zonal wind in January averaged for the years 1979–2015 (contours) and EMFC ($\times 10^5$ m s^{-2}; colors) for (a) the zonally averaged northern Atlantic (longitudes 0°–60°W) and (b) the zonally averaged northern Pacific (longitudes 150°E–120°W) calculated from the ERA-Interim data. Eddies are calculated using a Butterworth bandpass filter with a cutoff period of 3–10 days on 6-hourly data. The zonal wind contour interval (CI) is 5 m s^{-1}, where the thick contour is the zero-wind line and the dotted lines are for negative values.

gradients in the Pacific Ocean. They concluded that this trapping effect can suppress eddy activity in the baroclinic zone. In a later study, Nakamura and Shimpo (2004) showed that in the South Pacific winter, where the strong STJ traps eddy activity, the storm tracks are suppressed at the lower levels but not at the upper levels.

Brayshaw et al. (2008) investigated the sensitivity of eddies to changes in the SST gradient at different latitudes. They showed in an aquaplanet GCM that in the presence of a merged jet, eddies are most sensitive to changes in the SST gradient in the vicinity of the jet where baroclinicity is large, less sensitive when the SST gradient is modified in low latitudes (inside the Hadley cell), and least sensitive when the gradient was modified at high latitudes (significantly poleward of the jet maximum). In another study, Sampe et al. (2010) found that when a strong SST gradient (frontal SST gradient) exists in the vicinity of the jet, eddies are much stronger than the case when the gradient is flattened across a wider latitudinal range (but with a similar mean SST gradient). They concluded that a polar-front SST below the jet has a large effect on the storm tracks. These results are consistent with the idea that eddies are most sensitive to baroclinicity changes where it is already large and not to the mean baroclinicity (Yuval and Kaspi 2016, 2017).

Lachmy and Harnik (2014) showed in a two-layer quasigeostrophic (QG) model that the transition between a merged jet and an STJ is accompanied by a significant change in the waves' spectrum. They found that while a merged jet is dominated by wavenumbers 4–6, an STJ is dominated by longer waves (wavenumbers 1–3) with a weaker amplitude. Furthermore, Lachmy and Harnik (2014) suggested that in the STJ regime, eddies are weak despite the strong STJ shear, since the potential vorticity gradient does not change sign in the jet's vicinity, and therefore, the Charney and Stern (1962) criterion is not satisfied.

This study follows on the results of Yuval and Kaspi (2017) that studied the relation between the mean available potential energy (MAPE) and eddy kinetic energy (EKE) when the vertical and meridional temperature structures of the atmosphere changes. There, it was found that MAPE changes in the vicinity of the STJ cause relatively small changes in EKE compared to changes in the vicinity of the EDJ. The purpose of this study is to investigate the eddy sensitivity to jet amplitude and location changes in different circulation regimes (a merged-jet regime and a double-jet regime).

It is shown that in the extratropical region, eddies are most sensitive to changes in the temperature gradient in the vicinity of the EDJ and less sensitive to change in the poleward flank of the STJ, or significantly poleward of the EDJ core. In the tropical region, we find that eddies are also sensitive to changes in temperature gradient in the equatorward flank of the STJ (inside the tropics), although large temperature gradients inside the Hadley cell are not probable because of the large heat transport of the mean circulation that flattens efficiently the temperature gradient. Furthermore, it is demonstrated that when an atmospheric jet changes its characteristics and shifts equatorward (becomes more STJ-like), eddies tend to decrease.

The paper is organized as follows. Sections 2 discusses the GCM and the specific modifications to the Newtonian relaxation scheme used in the model (sections 2a and 2b), as well as how the temperature profiles of the reference states (section 2c) and the induced temperature profile modifications we study (section 2d) are obtained. In section 3, we present the results of the simulations, where we focus on the response of eddies to changes in the jets' amplitudes and locations. In section 4, the results and their implications are summarized.

2. Model description

a. Idealized GCM

A dry idealized GCM based on the spectral dynamical core of the Geophysical Fluid Dynamics Laboratory (GFDL) Flexible Modeling System (FMS) is used. All experiments are run with no topography, zonal asymmetries, or ocean. Linear damping of near-surface winds (below $\sigma = 0.7$) with a relaxation time of 1 day at the surface mimics turbulent dissipation in the boundary later [see Held and Suarez (1994) for details], and Newtonian relaxation of temperatures represents diabatic processes. All simulations have 60 vertical sigma levels (highest level is $\sigma = 0.004$) at T42 (2.8° × 2.8°). What distinguishes our simulations from Held and Suarez (1994) is the relaxation temperatures and the relaxation time used in the simulations, which are discussed in sections 2b, 2c, and 2d.

The simulations are integrated over 2000 days, where the first 400 days of each simulation are treated as spinup and the results are averaged over the last 1600 days. Only the Northern Hemisphere is presented in the figures, where in simulations that are hemispherically symmetric, the fields are averaged over both hemispheres.

b. Controlling the temperature profiles in the simulations

The diabatic heating formulation that was suggested by Zurita-Gotor (2007) is used in order to investigate the eddy sensitivity to changes in the vertical wind shear amplitude in the vicinity of the STJ and in the vicinity of the EDJ. In this heating scheme, the eddies and the zonal mean have different relaxation times. The temperature equation in this formulation can be written as

$$\partial_t T = \cdots - \alpha_T (T - \hat{T}) - \alpha_T \gamma (\hat{T} - T_R), \qquad (1)$$

where $\hat{T}$ is the zonal mean of field T, α_T is the relaxation frequency of eddies, and $\alpha_T\gamma$ is the relaxation frequency for the zonal mean state, where we take $\gamma = 100$, and T_R is the relaxation temperature. The fast relaxation for the zonal mean state is chosen to allow reproduction of any chosen target temperature profile with a good accuracy, such that the zonal- and time-mean temperature in a simulation is approximately the relaxation temperature. This allows us to systematically change the meridional temperature gradient at different latitudes and investigate how these changes affect the eddy fields.

It is important to note that using a prescribed mean temperature field in simulations does not mean that the resulting eddies are unrealistic or that there is no feedback between the eddy fields and the mean state. For example, surface wind, which affects the meridional wind gradient, is not determined by the mean temperature. Furthermore, a previous study by Chang (2006) showed that when the diabatic heating is tuned to reproduce a 3D Earthlike temperature field in an idealized GCM, the resulting eddy fields are qualitatively similar to eddy fields obtained from reanalysis data. This implies that a method where the temperatures are "prescribed" can produce a realistic circulation regime both for the mean and eddy fields. It is conceptually useful to consider the method that was used by Lunkeit et al. (1998), Chang (2006), and Yuval and Kaspi (2016), which calculates the diabatic heating profile that is necessary to produce a chosen target temperature, not as a method that prescribes the mean state but as a method prescribing a diabatic heating (and that the resulting temperature gradient is a consequence of this heating). In appendix B of Yuval and Kaspi (2017), we show that when the temperature is modified in a reference simulation, this method yields similar eddy field differences as the method used here. Therefore, we find both methods equally useful. A further discussion regarding the possible drawbacks of strong zonal temperature relaxation can be found in Yuval and Kaspi (2017).

c. Reference states of the atmosphere

Two different reference simulations are investigated in this study: one that has a single merged jet and another with two separate jets. It is beneficial to study two different reference simulations because it makes it possible to test the robustness of the results for different mean states.

The first reference temperature T_{HS}, which is referred as the merged-jet reference, is the equilibrium temperature structure of a simulation performed using the Held and Suarez (1994) forcing. The only difference between the current simulation and the Held and Suarez (1994) simulation is that the current one includes a dry convection scheme. The convection scheme relaxes the atmosphere to a lapse rate of $0.7\Gamma_{\mathrm{dry}}$, where $\Gamma_{\mathrm{dry}} = g/c_p$ is the dry adiabatic lapse rate on a short time scale of 4 h in cases when the lapse rate exceeds this value. The convection scheme is only used in order to obtain this reference temperature, and there is no convection scheme in any other simulation in this study. In simulations where this reference temperature is used, the eddy relaxation time α_T [see Eq. (1)] is the same as in Held and Suarez (1994).

The left panels of Fig. 2 show the temperature, wind, mass streamfunction, absolute angular momentum, EKE, eddy heat flux (EHF), and EMFC of the merged-jet reference. In the merged-jet reference, a single merged jet is obtained (see colors in Fig. 2a). This jet can be classified as a merged jet because it has two different driving mechanisms. In its center/poleward flank, there is significant EMFC, and it is located in the Ferrel cell (Figs. 2c,e), implying that in this region, it is an EDJ. On the other hand, its equatorward flank is found near the Hadley cell edge; it has a very baroclinic structure, and EMF divergence occurs there (Fig. 2e), which implies that at low latitudes it is a subtropical-like jet. The jet in the merged-jet reference is qualitatively similar to the jet over the northern Pacific in January (Fig. 1b). Figure 2c shows that an air parcel that flows poleward in the Hadley cell does not conserve its angular momentum since streamlines cross absolute angular momentum contours, and in addition, there is significant EMF divergence that occurs inside the Hadley cell.

The second reference temperature T_{April}, which is referred to as the separated-jet reference, is obtained by zonally averaging the multiannual (1979–2010) National Centers for Environmental Prediction–National Center

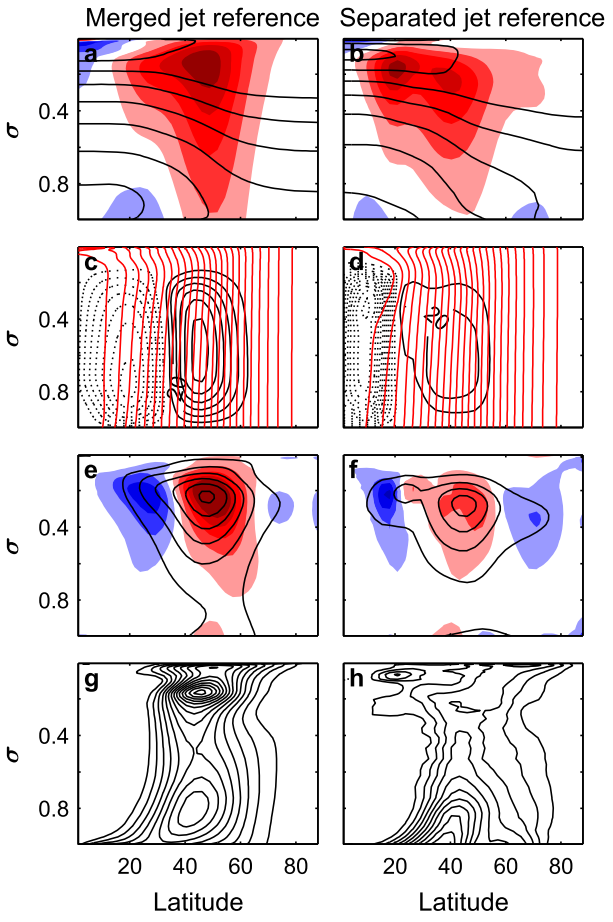

FIG. 2. Contours of (a),(b) temperature (CI = 15 K), (c), (d) mass streamfunction (black contours; CI = $10\,\mathrm{kg\,s^{-1}} \times 10^9$) and total angular momentum (red contours; CI = $0.04\Omega a^2$, where Ω is the rotation rate and a is the radius), (e),(f) EKE (CI = $50\,\mathrm{m^2\,s^{-2}}$) and (g),(h) EHF (CI = $2\,\mathrm{K\,m\,s^{-1}}$) for the (left) merged-jet and (right) separated-jet reference simulations. The zonal wind is plotted in colors in (a) and (b) (color spacing = $8\,\mathrm{m\,s^{-1}}$), and the meridional EMFC $\times 10^6$ is plotted in color in (e) and (f) (color spacing = $12\,\mathrm{m\,s^{-2}}$).

for Atmospheric Research (NCEP–NCAR) reanalysis April temperature above the northern Pacific basin (160°E–138°W).[1] This (zonally symmetric) reference temperature is chosen because it simulates an atmospheric state with two separate jets. We stress that the use of a realistic temperature does not mean that other atmospheric fields will be quantitatively realistic because of the idealized framework we use (lack of moisture, ocean, orography, etc.). The eddy relaxation time used in the simulations with the separated-jet reference is 20 days (uniform in space). The right panels of Fig. 2 show the Northern Hemisphere temperature, wind, mass streamfunction, absolute angular momentum, EKE, EHF, and EMFC of the separated-jet reference. Two separate jets are present in this simulation (Fig. 2b, colors): an STJ, which peaks at latitude 21°N close to the edge of the Hadley cell (Fig. 2d), and an EDJ, which peaks in the middle of the Ferrel cell at latitude 41°N, where EMFC occurs (Fig. 2f, colors). Note that the jet in this reference is quantitatively similar to the jet over the northern Atlantic in January (Fig. 1a). The eddy fields of the separated-jet reference shown in Figs. 2d, 2f, and 2h are weaker than the eddy fields in the merged-jet reference, which are plotted in Figs. 2c. 2e, and 2g. The weak eddies, and specifically weak EMFC, lead to relatively weak surface winds in the separated-jet reference. Figure 2d shows that the upper branch of the Hadley circulation is close to being angular momentum conserving since it does not cross total angular momentum contours (red).

d. *Profile modifications in the simulations*

It is well established that both the meridional temperature gradient and the vertical temperature gradient (i.e., the lapse rate) have an effect on the stability of the atmosphere (Eady 1949; Hoskins and Valdes 1990). To isolate the effect of changes in the meridional temperature gradient from the vertical temperature gradient, the temperature field is modified such that the lapse rate is left unchanged, while the meridional temperature gradient is modified.

Changing the meridional temperature gradient leads to changes in the wind shear (by thermal wind balance), and therefore, we are able to modify the zonal wind at different latitudes systematically. The reference temperature was modified in the following ways:

- The temperature gradient was increased or decreased at a chosen latitudinal band. This causes a change in the mean temperature gradient and tends to increase or decrease the wind shear at the proximity of these latitudes.
- The mean temperature gradient was increased at a chosen latitudinal band and decreased at a different latitudinal band simultaneously, such that the gradient was locally modified but its global-mean value is approximately unmodified.

For the case in which the gradient of the relaxation temperature was modified by a constant over a latitudinal band, the relaxation temperature can be written as $T_{\mathrm{relaxation}}(\phi, \sigma) = T_{\mathrm{ref}}(\phi, \sigma) + \delta T(\phi, \sigma, \phi_1, \phi_2, B)$, where

[1] Since the GCM used in this study has a different vertical resolution than the NCEP–NCAR reanalysis data, the temperature fields are interpolated to the levels of the model.

$$\delta T(\phi,\sigma,\phi_1,\phi_2,B)=\begin{cases}0 & \text{for} \quad \phi<\phi_1\\ -B(\phi-\phi_1) & \text{for} \quad \phi_1<\phi<\phi_2,\ \sigma>0.2\\ -B(\phi_2-\phi_1) & \text{for} \quad \phi>\phi_2,\ \sigma>0.2\\ -B(\phi-\phi_1)\exp\left[-\dfrac{(\sigma-0.2)^2}{0.1^2}\right] & \text{for} \quad \phi_1<\phi<\phi_2,\ \sigma<0.2\\ -B(\phi_2-\phi_1)\exp\left[-\dfrac{(\sigma-0.2)^2}{0.1^2}\right] & \text{for} \quad \phi>\phi_2,\ \sigma<0.2,\end{cases}$$

and ϕ is latitude, σ is the vertical coordinate, and B is the change in the meridional temperature gradient between latitudes ϕ_1 and ϕ_2. The exponential decay at the high levels where $\sigma<0.2$ is present to limit the temperature changes to the troposphere. In all experiments, the gradient amplitude used was $B=\pm(2/8.5)$ K (° lat)$^{-1}$. The latitudes ϕ_1 and ϕ_2 used in sections 3a and 3b are described in the top section of Table 1.

In the merged-jet reference simulation, which is hemispherically symmetric, the gradient was modified in both hemispheres, and in the separated-jet reference simulation, which is not symmetric, only the Northern Hemisphere was modified. Figures 3a–d show the induced temperature changes (color) in simulations with the separated-jet reference where the temperature gradient was increased at different latitudes.

To demonstrate the relevance of the chosen meridional temperature gradient changes in the simulations to Earth's atmosphere, the zonal-mean temperature gradient differences between January and July in the Southern Hemisphere (Fig. 4a; data taken from the ECMWF reanalysis) are compared to the typical induced changes in the simulations (Fig. 4b; see caption for details). The amplitude of the temperature gradient changes in the two panels is similar. In addition, the shape of the induced temperature gradient in the simulation (uniform temperature gradient change at all tropospheric levels; Fig. 4b) is similar to the changes that are seen on Earth at midlatitudes (Fig. 4a). We conclude that the meridional temperature gradient changes in the simulations well represent the amplitude and shape of the changes that occur on Earth between different seasons.

To consider changes in the structure of the meridional temperature gradient without changes in the mean gradient, relaxation profiles with the temperature structure $T_{\text{relaxation}}(\phi,\sigma)=T_{\text{ref}}(\phi,\sigma)+\delta T(\phi,\sigma,\phi_1,\phi_2,B)-\delta T(\phi,\sigma,\phi_3,\phi_4,B)$ were used with the parameters $B=\pm(2/8.5)$ K (° lat)$^{-1}$. To investigate the eddy response to a latitudinal shift of the EDJ, the parameters ϕ_1, ϕ_2, ϕ_3, and ϕ_4 were chosen such that the EDJ was strengthened on one of its flanks and weakened on its other flank; this is described in the middle section of Table 1.

3. Results

Eddy amplitudes are evaluated by three different vertical mean eddy quantities: the EKE, the meridional component of the Eliassen–Palm (EP) flux (EP_y), and the vertical component of the EP flux (EP_z). They can be explicitly expressed as (Andrews et al. 1983)

$$\text{EP}_y=\frac{\cos\phi}{\pi}(-\overline{u'v'}+\psi\partial_p\overline{u}) \tag{2}$$

and

$$\text{EP}_z=\frac{a\cos\phi}{\overline{p_s}}\left\{-\overline{u'w'}-\psi\left[\frac{\partial_\phi(\overline{u}\cos\phi)}{a\cos\phi}-f\right]\right\}, \tag{3}$$

where $\overline{A}$ is the zonal and time mean of field A; $\psi=\overline{v'\theta'}/\partial_p\overline{\theta}$; θ is the potential temperature; p is the pressure; $\overline{p_s}$ is the mean surface pressure; ϕ is the latitude; f is the Coriolis parameter; a is the planetary radius; and u, v, and w are the zonal, meridional, and vertical velocities, respectively. In the above equations, we rescaled the EP components by $a\pi$ and by $\overline{p_s}$, respectively, such that they will have the same units. All vertically mean quantities in this section are averaged in sigma coordinates between $0.2<\sigma<1$.

a. Case I: Separated jets

The temperature, zonal wind, mass streamfunction, and EKE are plotted in Fig. 3 for simulations where the temperature gradient was increased in the vicinity of the STJ (left column), between the jets (second column), in

TABLE 1. The experiments performed in this study. Numbers indicate the latitudes where the meridional temperature gradient was modified in the simulations. The changes are for both references unless otherwise noted.

Experiment description	Latitude changes at
Increasing or decreasing the mean temperature gradient between two latitudes (ϕ_1, ϕ_2)	(13°, 21°), (15°, 23°), (18°, 26°), (21°, 29°), (24°, 32°), (26°, 34°), (29°, 37°), (32°, 40°), (35°, 43°), (37°, 45°), (40°, 48°), (43°, 51°), (46°, 54°), (49°, 57°), (52°, 60°), (55°, 63°), (57°, 65°), (60°, 68°)
Shifting-jet simulations—changes at four latitudes (ϕ_1, ϕ_2, ϕ_3, ϕ_4)	(27°, 35°, 38°, 46°), (29°, 37°, 41°, 49°), (32°, 40°, 43°, 51°), (35°, 43°, 46°, 54°), (38°, 46°, 49°, 57°), (41°, 49°, 51°, 59°)
Changing jets amplitude simultaneously—changes at four latitudes (ϕ_1, ϕ_2, ϕ_3, ϕ_4)	Separated-jet reference (18°, 26°, 35°, 43°), (24°, 32°, 32°, 40°), (18°, 26°, 32°, 40°) Merged-jet reference (24°, 32°, 40°, 48°)

the vicinity of the EDJ (third column), and poleward of the EDJ for the separated-jet reference. Contours show the reference state, and colors show deviation from the reference. The EKE and EMFC are more sensitive to gradient changes in the vicinity of the EDJ than to changes in the vicinity of the STJ (Figs. 3m,o,q,s). For an increase in the temperature gradient in the vicinity of the EDJ (third column in Fig. 3), the surface wind increases at midlatitudes as a result of an increase in the EMFC (and decreases in lower latitudes where EMF divergence increases). When the meridional temperature gradient is increased in the vicinity of the STJ (two left columns in Fig. 3), there is no increase in surface winds at low latitudes since EMF does not converge at low latitudes. The small increase in surface wind in these simulations occurs at higher latitudes where there is an increase in EMFC.

To test if the large-eddy response to changes in the meridional temperature gradient in the vicinity of the EDJ is dependent on the exact latitudinal location of the modification in the gradient, a set of simulations was conducted where the meridional temperature gradient was modified at different latitudinal bands. The Northern Hemispheric mean of the EKE and EP fluxes differences between the separated-jet reference and these simulations are plotted in Fig. 5, where Figs. 5a and 5b are for the case where the gradient was increased and Figs. 5c and 5d are for a decreased gradient.[2] The abscissa shows the center latitude where the gradient was changed [defined as $(\phi_1 + \phi_2)/2$, where ϕ_1 and ϕ_2 are the boundaries of the latitudinal band that is changed; the latitudinal width of the change is always about 8.5°], and the ordinate shows the change in magnitude averaged over the whole Northern Hemisphere. When the meridional temperature gradient is increased in the vicinity of the EDJ, the change in EKE is maximal (Fig. 5a). The EKE is less sensitive to increase in the equatorward flank of the STJ (inside the tropics), even less sensitive to changes poleward of the EDJ, and even less sensitive (and can even have a decrease in EKE) when the gradient is increased at the latitudes between the jets. In the appendix, we show that when the amplitudes of the two jets are modified simultaneously, but with opposite signs, the eddy response is similar to the change in the EDJ (if the EDJ is stronger, eddy fields are also stronger).

Brayshaw et al. (2008) studied the response of eddy fields to changes in the position of the SST gradient. Their results are consistent with the results presented here in the sense that eddy fields are more sensitive to changes in the temperature gradient (SST gradient or tropospheric temperature gradient) when they are near the EDJ region, less sensitive to gradient changes at low latitudes inside the tropics, and even less sensitive to changes at high latitudes (significantly poleward of the jet maximum).

In general, the response of the EP fluxes is similar to the response of the EKE (Fig. 5b) but with the exception that when the gradient is increased at lower latitudes, the response in the meridional EP flux is opposite to the EKE response, and the response of the vertical EP flux is relatively weak. We note that a strong meridional temperature gradient is not likely to occur within the Hadley cell since the mean circulation tends to flatten the temperature gradient very efficiently. The response of eddies to a decreased temperature gradient is qualitatively similar, though a decreased gradient deep in the tropics results in similar magnitude eddy response as changes near the EDJ (Figs. 5c,d).

In Fig. 6, the temperature, zonal wind, EKE, EMFC, and EHF are plotted for simulations where the temperature gradient was modified such that the EDJ is shifted in latitude. When the EDJ is shifted poleward (left column),

[2] Averaging EKE in the vicinity of the EDJ (north and south of the center of the EDJ), instead of hemispheric averaging, yields similar qualitative results. Note that in some simulations, when the response around the EDJ is weak, there might be a sign difference between the hemispherically averaged change in EKE and the averaged EKE change in the vicinity of the EDJ. For example, in Fig. 3m, the EKE response in the vicinity of the EDJ is slightly more negative than positive, while the hemispherically integrated EKE is slightly positive, as indicated by the leftmost red dot in Fig. 5a.

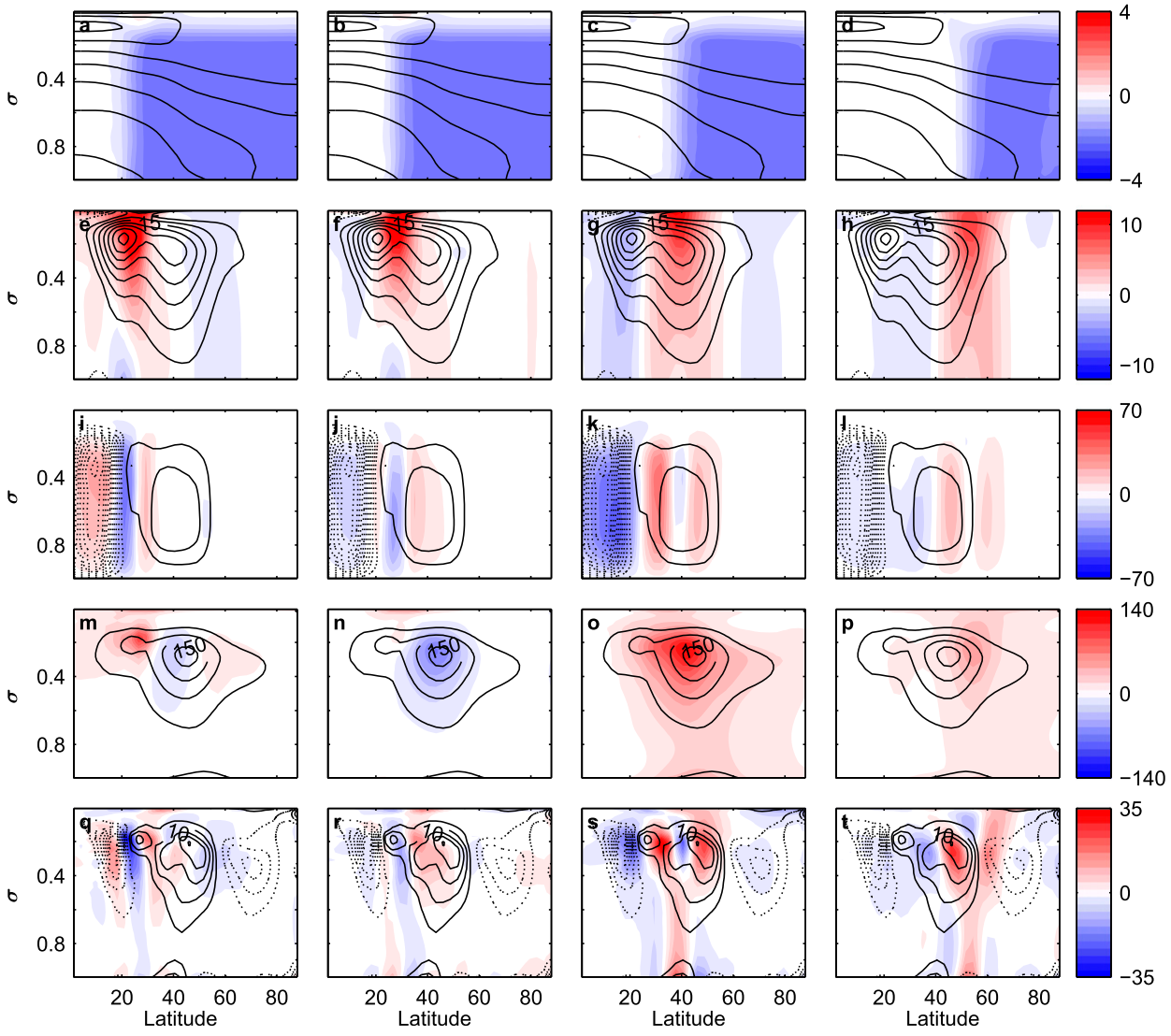

FIG. 3. (a)–(d) Temperature (CI = 15 K), (e)–(h) zonal wind (CI = 5 m s^{-1}), (i)–(l) mass streamfunction × 10^{-9} (CI = 10 kg s^{-1}), (m)–(p) EKE (CI = 50 m^2 s^{-2}), and (q)–(t) EMFC × 10^6 (CI = 5 m s^{-2}) for simulations where the meridional temperature gradient was (first column) in the vicinity of the STJ (latitudes 18°, 26°N), (second column) at the region between the jets (latitudes 24°, 32°N), (third column) at the EDJ region (latitudes 35°, 43°N), and (fourth column) poleward of the EDJ (latitudes 49°, 57°N). Contours show the separated-jet reference (dashed contours for negative values), and the colors represent deviation from this reference.

eddy fields tend to increase (Figs. 6e,g,i; though the EMFC shows a mixed response), and when the EDJ is shifted equatorward, the eddy fields tends to weaken (Figs. 6f,h,j). These results imply that when the jet becomes more EDJ-like (poleward shift), eddies tend to increase, and when it becomes more STJ-like (equatorward shift), eddies tend to decrease. The sensitivity of these results to the exact location of the center of the shift was examined in a series of simulations. It was found that when the jet is shifted poleward, if the latitude of the shift's center is equatorward of latitude 43°N, the eddies tend to strengthen, and otherwise, they weaken (the cases where the eddies weaken are cases that the shear decrease occurs close to the peak of the EDJ). When the jet is shifted equatorward, the eddies tend to weaken if the latitude of the shift's center is poleward of latitude 40°N, and otherwise, they tend to strengthen.

b. *Case II: Mixed jet*

The temperature, zonal wind, mass streamfunction, EKE, and EMFC are plotted in Fig. 7 for simulations where the temperature gradient was modified at different latitudes for the merged-jet background reference. Contours show the reference state, and colors show deviation from this reference. This figure shows that

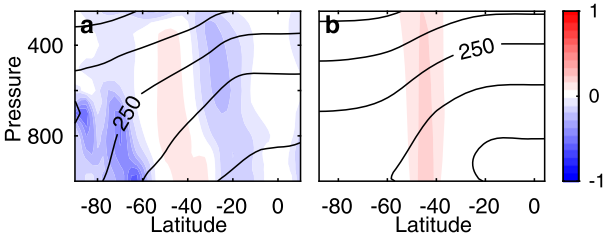

FIG. 4. The zonally averaged meridional temperature gradient difference [K (° lat)$^{-1}$; color] in the Southern Hemisphere (a) between January and July calculated from the ERA-Interim data and (b) for a simulation with increased temperature gradient at midlatitudes $(\phi_1, \phi_2) = (40.5°, 49°)$ to the merged-jet reference. Contours show the zonally averaged temperature distribution (CI = 20 K) in (a) January and (b) the merged-jet reference.

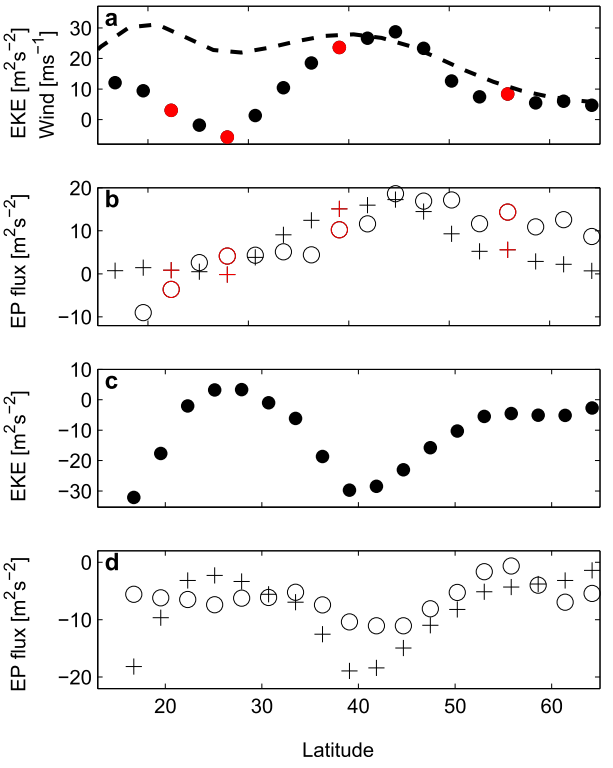

FIG. 5. (a) The zonal wind as a function of latitude at $\sigma = 0.25$ of the reference simulation (dashed line) and the Northern Hemispheric averaged EKE (dots; each dot represents a different simulation). The ordinate is the difference of the mean EKE from the separated-jet reference simulation, and the abscissa shows the center latitude where the temperature gradient was increased. The red dots are calculated from the simulations presented in Fig. 3. (b) As in (a), but calculated for the horizontal (×20; circles) and vertical (plus signs) rescaled EP flux [Eqs. (2) and (3)]. (c),(d) As in (a) and (b), respectively, but for simulations with a decreased gradient.

EKE is most sensitive to changes in the gradient in the vicinity of the EDJ (the EKE response in Fig. 7o is largest). Furthermore, when the temperature gradient is increased inside the Hadley cell (two left columns in Fig. 7), the Hadley cell strengthens and contracts. In this reference, an air parcel that moves poleward in the Hadley cell does not conserve its angular momentum (Fig. 2c), and EMF divergence acts to weaken the zonal wind. The increase of the Hadley cell amplitude with the increase of EMF divergence is consistent with the results of Walker and Schneider (2006), who showed that in cases where eddies play an important role in the Hadley cell, its strength is proportional to the EMF divergence. Furthermore, when the increase in temperature gradient occurs at low latitudes (Fig. 7, two left columns), the increase in surface winds (and in EMFC) occurs poleward of this region, where the Ferrel cell strengthens. This implies that even when the temperature gradient is increased inside the Hadley cell, the increase in surface winds (and EMFC) will not occur inside the Hadley cell [see also Lachmy and Harnik (2014) for a discussion why there is EMF divergence inside the Hadley cell].

Figures 8a and 8b show the globally averaged EKE and EP flux differences between simulations where the temperature gradient was increased (decreased gradient in Figs. 8c and 8d) at different latitudes and the merged-jet reference simulation as a function of the latitude where the temperature gradient was changed. The results shown in Fig. 8a are qualitatively similar to the results of section 3a. Eddies are found to be more sensitive to changes in the temperature gradient (or wind shear) in the vicinity of the EDJ, less sensitive to temperature gradient changes inside the Hadley cell, even less sensitive to changes in the gradient in high latitudes (poleward of the EDJ), and least sensitive (and can even show an opposite response) to changes on the equatorward flank of the EDJ (which is equivalent to the region between the jets that was found to be least sensitive in section 3a). In the merged-jet reference simulation, the Hadley cell's edge is at latitude $\phi_{\text{Hadley}} \approx 30°$N, and when the temperature gradient is modified deep in the tropics (below latitude 20°N), the change in the EKE can be as big as the change in EKE when the temperature gradient is modified in the vicinity of the EDJ (Fig. 8a). This implies that changes in the temperature gradient deep in the tropics can have a significant impact on eddies.

A significant difference between the results of the two references is the response of the EP fluxes when the temperature is increased at low latitudes (i.e., inside the Hadley cell). In the merged-jet reference, the response of eddy fluxes is similar to the response of the EKE (when the EKE increases more, so do eddy fluxes; Fig. 8), and in the separated-jet reference, an increase in the EKE is not always accompanied by an increase in the fluxes. For example, in the separated-jet simulations where the lower temperature gradient is increased inside the Hadley cell, the EKE increases (the points at lower latitudes in

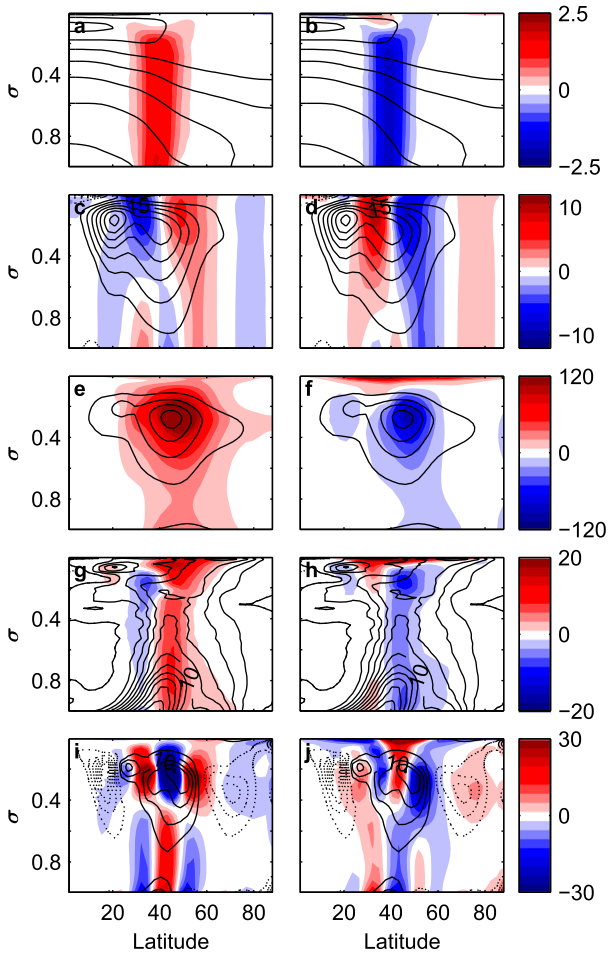

FIG. 6. (a),(b) Temperature (K), (c),(d) zonal wind ($m\,s^{-1}$), (e),(f) EKE ($m^2\,s^{-2}$), (g),(h) EHF ($m\,s^{-1}\,K$), and (i),(j) EMFC $\times$ 10^6 ($m\,s^{-2}$) for simulations where the EDJ was shifted (left) poleward and (right) equatorward. The meridional temperature gradient was changed at latitudes 30°–38° and 41°–49°N. Contours show the separated-jet reference (dashed contours for negative values), and the colors represent deviation from this reference. The CIs are 15 K (temperature), 5 $m\,s^{-1}$ (zonal wind), 50 $m^2\,s^{-2}$ (EKE), 2 $m\,s^{-1}$ K (EHF), and 5 $m\,s^{-2}$ (EMFC).

Fig. 5a), but eddy fluxes are unchanged or even decrease on average (Fig. 5b). The different eddy response is possibly related to the different nature of the Hadley cell in each of the reference simulations. In the merged-jet reference, eddies are dominant inside the Hadley cell, the mean angular momentum is not conserved on a poleward-moving air parcel, and EMF divergence occurs inside the cell, while in the separated-jet reference, the upper branch of the Hadley cell is almost angular momentum conserving, and eddies do not play a big role in the Hadley cell circulation (Figs. 2c,d). This possibly also results in the different response of the Hadley cell when the temperature gradient is modified at low latitudes; in the separated-jet reference, the mass streamfunction of the Hadley cell weakens and expands in a response to increased gradient at low latitudes (Fig. 3i), while in the merged-jet reference, the response is opposite (Figs. 7i,j).

The temperature, zonal wind, EKE, EMFC, and EHF are plotted in Fig. 9 for simulations in which the temperature gradient was modified such that the EDJ is shifted in latitude. A poleward shift of the EDJ results in an intensification of eddy fields, while an equatorward shift results in a decrease in eddy fields. These results are similar to what was shown in section 3b for the separated-jet reference. The sensitivity of these results to the exact location of the center of the shift was examined in a series of simulations, and it was found that when the jet is shifted poleward, if the latitude of the shift's center is equatorward of latitude 48°N, the eddies tend to strengthen and otherwise to weaken. When the jet is shifted equatorward, the eddies weaken if the latitude of the shift's center is poleward of latitude 43°N, and otherwise, they tend to strengthen.

When the temperature gradient is modified at a certain latitudinal band, the EKE response is over a broad range of latitudes. This effect is most obvious when the temperature gradient changes are found inside the Hadley cell and the EKE response happens at all midlatitudes (Fig. 7m). This implies that local baroclinicity measures are not sufficient to understand the local EKE response to changes in the meridional structure of the temperature gradient. In general, eddy fluxes and especially EHF show a more localized response than EKE when the temperature gradient is modified, although their response is not confined to the region where the gradient was changed.

4. Summary and discussion

The eddy response to changes in the vertical wind shear at different latitudes was investigated. We especially focus on the eddy sensitivity to jet amplitude changes in the vicinity of the STJ and the EDJ and the response of eddies to a jet shift. Understanding how different jet types affect eddy activity is important since it serves as a guideline for characterizing how unstable the atmosphere is also by considering the type of the jet and not only by linear baroclinicity measures.

To methodically modify the jet strength at different latitudes (while keeping the wind shear at other latitudes approximately unchanged), an idealized GCM was used with a Newtonian cooling scheme that relaxes the zonal-mean temperature field 100 times faster than it relaxes eddies. This allows us to control the zonal-mean temperature field with high accuracy and, since thermal wind balance approximately holds, to set the vertical wind shear.

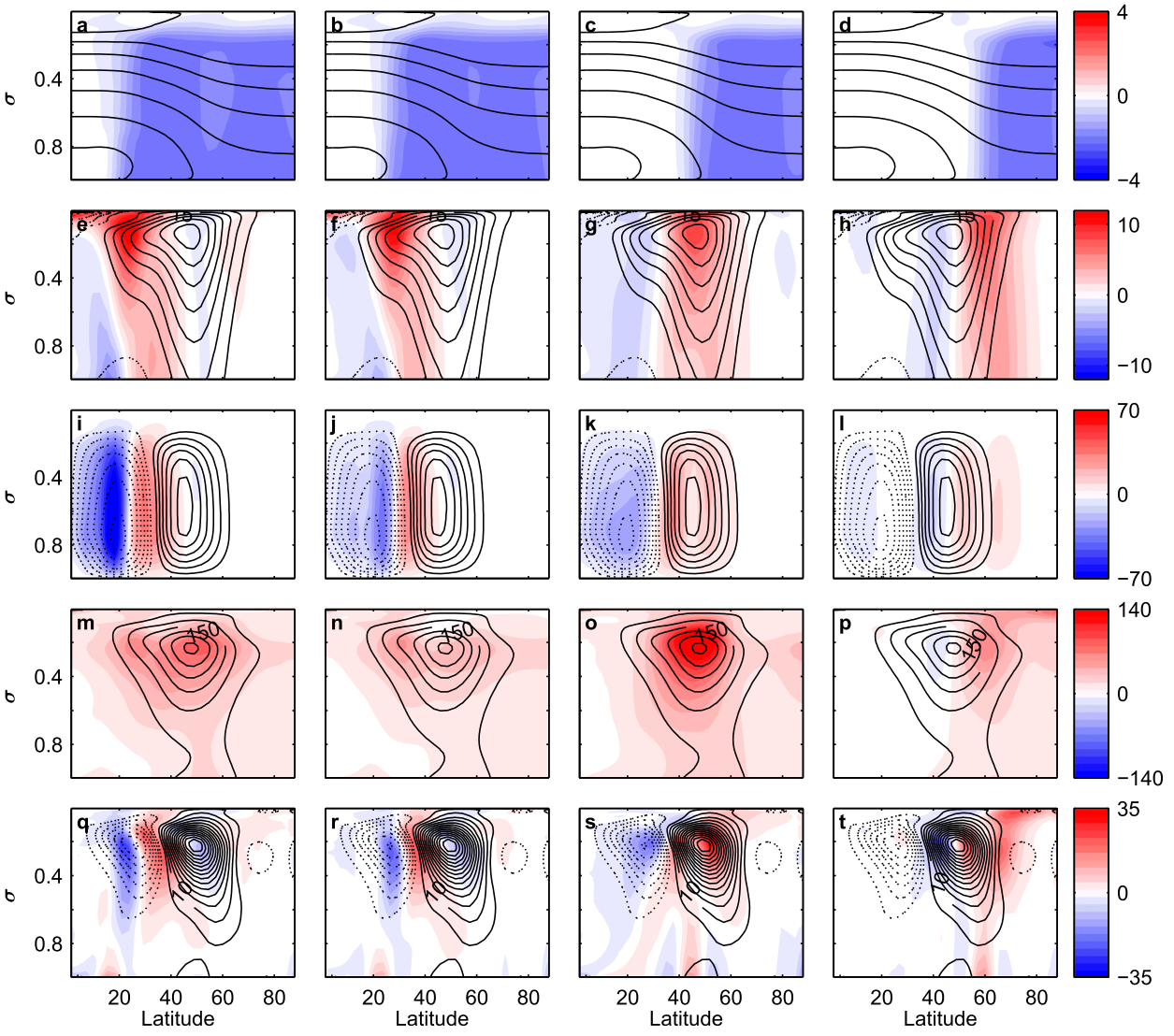

FIG. 7. (a)–(d) Temperature (K), (e)–(h) zonal wind ($m\,s^{-1}$), (i)–(l) mass streamfunction $\times 10^{-9}$ ($kg\,s^{-1}$), (m)–(p) EKE ($m\,s^{-2}$), and (q)–(t) EMFC $\times 10^{6}$ ($m\,s^{-2}$) for simulations where the meridional temperature gradient was increased (first column) in the tropics (latitudes 15°, 23°N), (second column) equatorward flank of the jet (latitudes 21°, 29°N), (third column) at the jet center (latitudes 41°, 49°N), and (fourth column) at the poleward flank of the jet (latitudes 55°, 63°N). Contours show the merged-jet reference (dashed contours for negative values), and the colors represent the deviation from this reference. The CIs are 15 K (temperature), $5\,m\,s^{-1}$ (zonal wind), $10\,kg\,s^{-1}$ (mass streamfunction), $50\,m^2\,s^{-2}$ (EKE), and $5\,m\,s^{-2}$ (EMFC).

To investigate the eddy response to changes in the jet structure, two different reference simulations were considered: one with a well-separated STJ and EDJ and the other with a single merged jet. It was found in both references that the eddy fields are most sensitive to changes in the temperature gradient in the vicinity of the EDJ, less sensitive to gradient changes in the equatorward flank of the STJ (latitudes inside the Hadley cell), even less sensitive to gradient changes significantly poleward of the EDJ, and least sensitive in cases where the gradient was modified between the jets (at the poleward flank of the STJ). In addition, it was found that when the STJ weakens and the EDJ strengthens simultaneously, eddies tend to intensify (see the appendix). In a different simulation set, it was shown that a moderate poleward (equatorward) shift of the EDJ tends to strengthen (weaken) eddy fields. Since the qualitative results of the simulations in the two references were similar, it increases the confidence that these results could be generalized and be applicable to other situations.

The results of this study has potentially important implications regarding the Pacific midwinter minimum

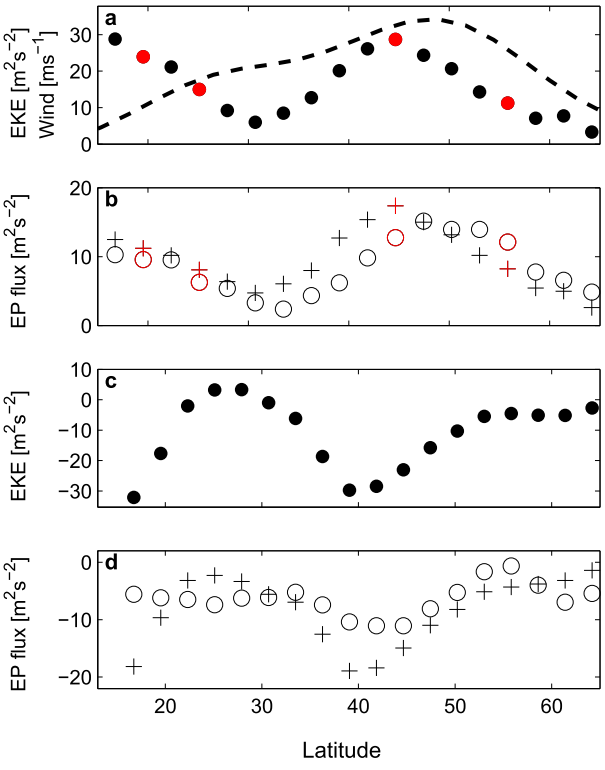

FIG. 8. As in Fig. 5, but dots represent the globally averaged EKE for the merged-jet simulations. The red dots are calculated from the simulations presented in Fig. 7.

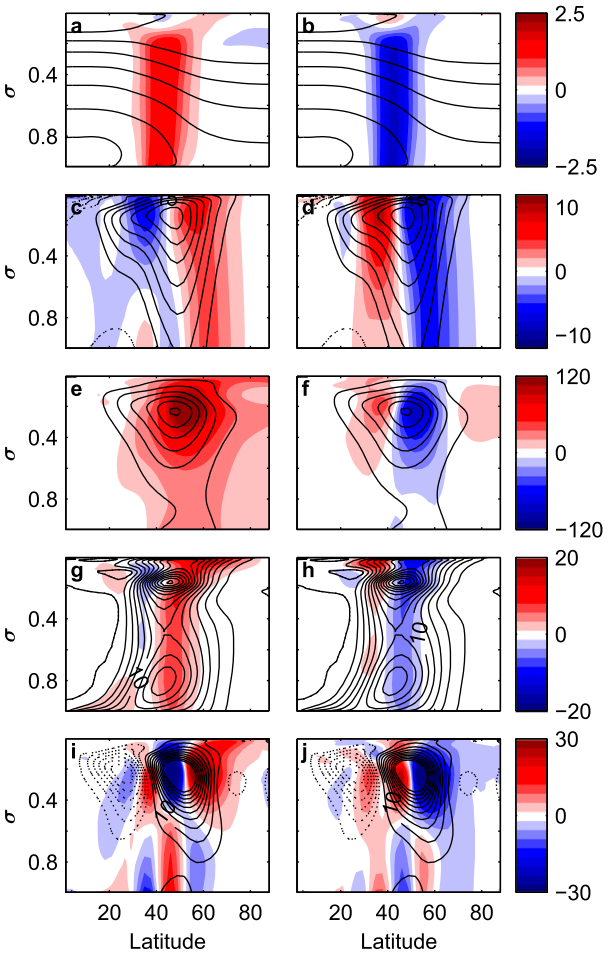

FIG. 9. As in Fig. 6, but the meridional temperature gradient was changed at latitudes 32°–40° and 43°–51°N using the merged-jet reference. Contours show the merged-jet reference (dashed contours for negative values), and the colors represent deviation from this reference.

(MWM) in EKE (Nakamura 1992). The presence of the Pacific MWM is inconsistent with theoretical expectations since baroclinicity measures are on average largest in January but the EKE is at a local minimum during midwinter. The results of this study imply that the presence of the MWM might be related to the jet transition that occurs in the Pacific. During winter, there is a strong Hadley cell, the Pacific jet is found at low latitudes, and it is in a merged-jet state (similar to the merged-jet state in this study). On the other hand, during transition seasons, the jet is found at higher latitudes and resembles an eddy-driven jet. As shown in this study, eddies tend to be stronger when the jet resembles an EDJ than when it resembles an STJ. Combining this result with the changes in the jet characteristics in winter compared to transition seasons could potentially explain the presence of the MWM.

In a related study (Yuval et al. 2018, manuscript submitted to *Geophys. Res. Lett.*), we further discuss the effect of the jet characteristics on the presence of the Pacific MWM. We find that when a zonally symmetric Pacific temperature distribution is simulated, an MWM-like behavior that resembles reanalysis data is obtained. This implies that the Pacific temperature distribution and its resulting jet structure in the different seasons are sufficient to explain the MWM. Furthermore, we show in reanalysis data that when the Pacific winter jet is found at lower latitudes during winter (and more resembles an STJ), the EKE is weaker than when the jet is located more poleward. These results are consistent with the findings of the present paper.

A potential mechanism that was not discussed here, and might influence baroclinic growth in midlatitudes, is the barotropic governor (James and Gray 1986; James 1987). According to this mechanism, a concentration of barotropic shear could have a damping effect on baroclinic eddies, and therefore, sharp jets in the meridional direction could be less favorable for baroclinic eddies than wider jets. This implies that when the jet amplitude is increased near its maximum (and the jet becomes sharper), barotropic shear is more concentrated and can

weaken eddies compared to the case where the jet amplitude is increased near its flanks and the meridional temperature gradient of the zonal wind is less concentrated. However, this effect is not the dominant effect in these simulations, since the eddies' response is larger when the gradient is modified in the vicinity of the EDJ maximum and less sensitive to changes near its flanks (Figs. 3o, 5a, 7o, and 8a). If the barotropic governor is the dominant mechanism, we would expect the result to be opposite.

Acknowledgments. This research has been supported by the Israeli Science Foundation (Grant 1819/16).

APPENDIX

Modifying the Jets' Strength Simultaneously

A complementary experiment was conducted for the purpose of studying the eddy response to simultaneous changes in the jets' magnitude where the parameters ϕ_1, ϕ_2, ϕ_3, and ϕ_4 were chosen such that the jets would change their magnitude in an opposite manner and are described in the bottom section of Table 1. We note that the chosen latitudes for the merged-jet reference were different from the separated-jet reference since the jet location is more poleward than in the separated-jet reference case.

Figure A1 shows the temperature (Figs. A1a,b); zonal wind (Figs. A1c,d); and response of the EKE (Figs. A1e,f), EHF (Figs. A1g,h), and EMFC (Figs. A1i,j) to simultaneous wind changes in the EDJ and STJ for the separated-jet reference. When the jets are modified simultaneously, but with opposite tendencies, eddies are more affected by the change in the EDJ (if the EDJ is strengthened, so are the eddies, and vice versa). This result is consistent with the results in Fig. 5, where it is shown that eddies are more sensitive to meridional gradient changes in the vicinity of the EDJ than near the STJ. The results are shown for gradient modifications at latitudes $(\phi_1, \phi_2, \phi_3, \phi_4) \approx (18°, 26°, 35°, 43°\text{N})$, but the results are qualitatively similar for other parameters shown in Table 1 (bottom section). Similar simulations with the merged-jet reference were conducted. In these simulations, the equatorward flank of the jet, which is subtropical-like (EMF divergence occurs there, and it is found near the Hadley cell edge), was strengthened (weakened), and the jet core, which is eddy-driven-like (EMFC occurs in the jet core), was weakened (strengthened) simultaneously. It was found that eddy fields are more sensitive to changes in the jet core than in the equatorward flank of the jet (not shown).

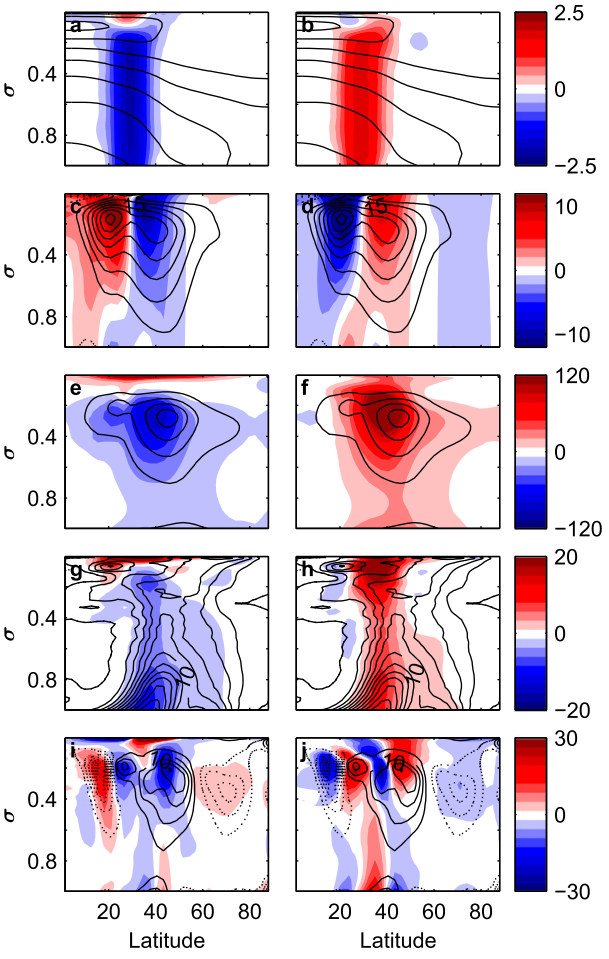

FIG. A1. As in Fig. 6, but the temperature gradient was (left) increased near the STJ and decreased near the EDJ and (right) decreased near the STJ and increased near the EDJ.

REFERENCES

Andrews, D. G., J. D. Mahlman, and R. W. Sinclair, 1983: Eliassen-Palm diagnostics of wave–mean flow interaction in the GFDL "SKYHI" general circulation model. *J. Atmos. Sci.*, **40**, 2768–2784, https://doi.org/10.1175/1520-0469(1983)040<2768:ETWATM>2.0.CO;2.

Brayshaw, D. J., B. Hoskins, and M. Blackburn, 2008: The storm-track response to idealized SST perturbations in an aqua-planet GCM. *J. Atmos. Sci.*, **65**, 2842–2860, https://doi.org/10.1175/2008JAS2657.1.

Chang, E. K. M., 2006: An idealized nonlinear model of the Northern Hemisphere winter storm tracks. *J. Atmos. Sci.*, **63**, 1818–1839, https://doi.org/10.1175/JAS3726.1.

Charney, J. G., and M. E. Stern, 1962: On the stability of internal baroclinic jets in a rotating atmosphere. *J. Atmos. Sci.*, **19**, 159–172, https://doi.org/10.1175/1520-0469(1962)019<0159:OTSOIB>2.0.CO;2.

Eady, E. T., 1949: Long waves and cyclonic waves. *Tellus*, **1** (3), 33–52, https://doi.org/10.3402/tellusa.v1i3.8507.

Eichelberger, S. J., and D. L. Hartmann, 2007: Zonal jet structure and the leading mode of variability. *J. Climate*, **20**, 5149–5163, https://doi.org/10.1175/JCLI4279.1.

Held, I. M., 1975: Momentum transport by quasi-geostrophic eddies. *J. Atmos. Sci.*, **32**, 1494–1497, https://doi.org/10.1175/1520-0469(1975)032<1494:MTBQGE>2.0.CO;2.

——, and A. Y. Hou, 1980: Nonlinear axially symmetric circulations in a nearly inviscid atmosphere. *J. Atmos. Sci.*, **37**, 515–533, https://doi.org/10.1175/1520-0469(1980)037<0515:NASCIA>2.0.CO;2.

——, and M. J. Suarez, 1994: A proposal for the intercomparison of the dynamical cores of atmospheric general circulation models. *Bull. Amer. Meteor. Soc.*, **75**, 1825–1830, https://doi.org/10.1175/1520-0477(1994)075<1825:APFTIO>2.0.CO;2.

Hoskins, B. J., and P. J. Valdes, 1990: On the existence of storm-tracks. *J. Atmos. Sci.*, **47**, 1854–1864, https://doi.org/10.1175/1520-0469(1990)047<1854:OTEOST>2.0.CO;2.

James, I. N., 1987: Suppression of baroclinic instability in horizontally sheared flows. *J. Atmos. Sci.*, **44**, 3710–3720, https://doi.org/10.1175/1520-0469(1987)044<3710:SOBIIH>2.0.CO;2.

——, and L. J. Gray, 1986: Concerning the effect of surface drag on the circulation of a baroclinic planetary atmosphere. *Quart. J. Roy. Meteor. Soc.*, **112**, 1231–1250, https://doi.org/10.1002/qj.49711247417.

Lachmy, O., and N. Harnik, 2014: The transition to a subtropical jet regime and its maintenance. *J. Atmos. Sci.*, **71**, 1389–1409, https://doi.org/10.1175/JAS-D-13-0125.1.

Lee, S., and H. Kim, 2003: The dynamical relationship between subtropical and eddy-driven jets. *J. Atmos. Sci.*, **60**, 1490–1503, https://doi.org/10.1175/1520-0469(2003)060<1490:TDRBSA>2.0.CO;2.

Lunkeit, F., L. Fraedrich, and S. E. Bauer, 1998: Storm tracks in warmer climate: Sensitivity studies with a simplified global circulation model. *Climate Dyn.*, **14**, 813–826, https://doi.org/10.1007/s003820050257.

Nakamura, H., 1992: Midwinter suppression of baroclinic wave activity in the Pacific. *J. Atmos. Sci.*, **49**, 1629–1642, https://doi.org/10.1175/1520-0469(1992)049<1629:MSOBWA>2.0.CO;2.

——, and T. Sampe, 2002: Trapping of synoptic-scale disturbances into the North-Pacific subtropical jet core in midwinter. *Geophys. Res. Lett.*, **29**, 1761, https://doi.org/10.1029/2002GL015535.

——, and A. Shimpo, 2004: Seasonal variations in the Southern Hemisphere storm tracks and jet streams as revealed in a reanalysis dataset. *J. Climate*, **17**, 1828–1844, https://doi.org/10.1175/1520-0442(2004)017<1828:SVITSH>2.0.CO;2.

Panetta, R. L., 1993: Zonal jets in wide baroclinically unstable regions: Persistence and scale selection. *J. Atmos. Sci.*, **50**, 2073–2106, https://doi.org/10.1175/1520-0469(1993)050<2073:ZJIWBU>2.0.CO;2.

Rhines, P. B., 1975: Waves and turbulence on a beta plane. *J. Fluid Mech.*, **69**, 417–443, https://doi.org/10.1017/S0022112075001504.

Sampe, T., H. Nakamura, A. Goto, and W. Ohfuchi, 2010: Significance of a midlatitude SST frontal zone in the formation of a storm track and an eddy-driven westerly jet. *J. Climate*, **23**, 1793–1814, https://doi.org/10.1175/2009JCLI3163.1.

Son, S.-W., and S. Lee, 2005: The response of westerly jets to thermal driving in a primitive equation model. *J. Atmos. Sci.*, **62**, 3741–3757, https://doi.org/10.1175/JAS3571.1.

Vallis, G. K., 2006: *Atmospheric and Oceanic Fluid Dynamics.* Cambridge University Press, 770 pp.

Walker, C. C., and T. Schneider, 2006: Eddy influences on Hadley circulations: Simulations with an idealized GCM. *J. Atmos. Sci.*, **63**, 3333–3350, https://doi.org/10.1175/JAS3821.1.

Yuval, J., and Y. Kaspi, 2016: Eddy activity sensitivity to changes in the vertical structure of baroclinicity. *J. Atmos. Sci.*, **73**, 1709–1726, https://doi.org/10.1175/JAS-D-15-0128.1.

——, and ——, 2017: The effect of vertical baroclinicity concentration on atmospheric macroturbulence scaling relations. *J. Atmos. Sci.*, **74**, 1651–1667, https://doi.org/10.1175/JAS-D-16-0277.1.

Zurita-Gotor, P., 2007: The relation between baroclinic adjustment and turbulent diffusion in the two-layer model. *J. Atmos. Sci.*, **64**, 1284–1300, https://doi.org/10.1175/JAS3886.1.